



Novel triplex nucleic acid lateral flow immunoassay for rapid detection of Nipah virus, Middle East respiratory syndrome coronavirus and Reston ebolavirus

Santhalembi Chingtham^{1,2}, Diwakar D. Kulkarni¹, Sumi Sivaraman³, Anamika Mishra¹, Atul K. Pateriya¹, Vijendra Pal Singh¹ and Ashwin Ashok Raut^{1*} 

Abstract

We report the development of a triplex nucleic acid lateral flow immunoassay (NALFIA) for the detection of the genomes of Nipah virus (NiV), Middle East respiratory syndrome coronavirus (MERS-CoV) and Reston ebolavirus (REBOV), which are intended for screening bats as well as other hosts and reservoirs of these three viruses. Our triplex NALFIA is a two-step assay format: the target nucleic acid in the sample is first amplified using tagged primers, and the tagged dsDNA amplicons are captured by antibodies immobilized on the NALFIA device, resulting in signal development from the binding of a streptavidin-colloidal gold conjugate to a biotin tag on the captured amplicons. Triplex amplification of the *N* gene of NiV, the *UpE* gene of MERS-CoV, and the *Vp40* gene of REBOV was optimized, and three compatible combinations of hapten labels and antibodies were identified for end point detection. The lowest RNA copy numbers detected by the triplex NALFIA were 8.21e4 for the NiV *N* target, 7.09e1 for the MERS-CoV *UpE* target, and 1.83e4 for the REBOV *Vp40* target. Using simulated samples, the sensitivity and specificity for MERS-CoV and REBOV targets were estimated to be 100%, while the sensitivity and specificity for the NiV target were 91% and 93.3%, respectively. The compliance rate between triplex NALFIA and real-time RT-PCR was 92% for the NiV *N* target and 100% for the MERS-CoV *UpE* and REBOV *Vp40* targets.

Keywords Nucleic acid lateral flow immunoassay (NALFIA), Nipah virus, Middle East respiratory syndrome coronavirus, Reston ebolavirus

Handling editor: Zutao Zhou.

*Correspondence:

Ashwin Ashok Raut
ashwinraut73@gmail.com

¹ Pathogenomics Laboratory, ICAR-National Institute of High Security Animal Diseases, Bhopal, Madhya Pradesh 462022, India

² Division of Veterinary Virology, ICAR-Indian Veterinary Research Institute, Nainital, Uttarakhand 263138, India

³ Ubio Biotechnology Systems Pvt. Ltd., Cochin, Kerala 683503, India

Introduction

The devastating implications of emerging zoonotic infectious diseases are well recognized. Nipah virus (NiV), Middle East respiratory syndrome coronavirus (MERS-CoV) and ebolaviruses are emerging zoonotic viruses that cause high fatality rates in humans, incur economic losses and affect international travel and animal trade due to livestock involvement (Chua et al. 2000; Zaki et al. 2012; Leroy et al. 2005). Reston ebolavirus (REBOV) is nonlethal to humans (Miranda et al. 1991; Marsh et al. 2011); however, the high pathogenicity of REBOV in nonhuman primates, the nonclinical susceptibility of domestic



© The Author(s) 2024. **Open Access** This article is licensed under a Creative Commons Attribution 4.0 International License, which permits use, sharing, adaptation, distribution and reproduction in any medium or format, as long as you give appropriate credit to the original author(s) and the source, provide a link to the Creative Commons licence, and indicate if changes were made. The images or other third party material in this article are included in the article's Creative Commons licence, unless indicated otherwise in a credit line to the material. If material is not included in the article's Creative Commons licence and your intended use is not permitted by statutory regulation or exceeds the permitted use, you will need to obtain permission directly from the copyright holder. To view a copy of this licence, visit <http://creativecommons.org/licenses/by/4.0/>. The Creative Commons Public Domain Dedication waiver (<http://creativecommons.org/publicdomain/zero/1.0/>) applies to the data made available in this article, unless otherwise stated in a credit line to the data.

pigs and humans to REBOV infection, and the prevalence of REBOV in Asia, unlike other ebolaviruses that are confined to a particular geographical area outside Asia (Taniguchi et al. 2011; Jayme et al. 2015; Barrette et al. 2009; Demetria et al. 2018), suggest the possibility of the emergence of mutant REBOV with increased lethality in humans and livestock. Bats are reservoirs of henipaviruses, coronaviruses and ebolaviruses, although direct or indirect involvement of bats in MERS-CoV transmission has yet to be identified (Halpin et al. 2011; Pourrut et al. 2009; Ithete et al. 2013; Geldenhuys et al. 2013; Annan et al. 2013; Yang et al. 2014). Therefore, it is imperative to screen reservoir bats for the assessment of potential health risks and threats imposed by NiV, MERS-CoV and REBOV in Asia. The present study highlights the development of a triplex one-step RT-PCR-based triplex nucleic acid lateral flow immunoassay (NALFIA) for rapid and simultaneous screening of NiV, MERS-CoV and REBOV samples, particularly from bats, by targeting viral RNA. Multiplexing allows the use of a single sample for screening of multiple pathogens in a single test, hence making the assay rapid and cost-effective and reducing the need for multiple sample processing from an individual animal to test multiple pathogens, a consideration vital to screening wildlife (bat) samples.

For the detection of viral infections, molecular tests are superior to nonnucleic acid diagnostic tests such as serology and microscopy in terms of sensitivity and specificity (Crannell et al. 2016). Conventional PCR-based tests are sensitive; however, end-point detection of PCR amplicons by agarose gel electrophoresis is complex considering the operation, hazard, time and cost. While the real-time PCR system does not require an additional post-run wet laboratory procedure, its disadvantages are its high cost and sophistication, which limit its usage in low-resource settings. An efficient alternative readout system is the NALFIA, which is a subtype of the lateral flow assay (LFA) (Damborský et al. 2016). NALFIA uses an immobilized antibody to capture double-stranded DNA amplicons through a tag on one of the oligo primers. Another tag is incorporated into the amplicon through one of the primers, which has affinity for the detector conjugate, the interaction of which creates the signal on the test line and the conjugate control line. Therefore, NALFIA can also be interpreted as a two-step assay in which the target nucleic acid in the sample is first amplified, followed by the examination of amplicons on the LFA device. The NALFIA device offers increased ease of operation of the PCR setup and rapid and safe detection of the amplified products of the viral genome. PCR-based monoplex or multiplex NALFIAs for the detection of DNA targets have been reported in previous studies (Crannell et al. 2016; Mens et al. 2012a, b; Kamphée

et al. 2015). Recently, isothermal assay-based multiplex NALFIAs have also been developed for the detection of SARS-CoV-2 RNA (Zhu et al. 2020; Zhang et al. 2021; Jia et al. 2021).

We report the development of a triplex one-step RT-PCR-based NALFIA with three test lines and a conjugate control line for simultaneous detection of NiV, MERS-CoV and REBOV RNA targets. The oligonucleotide primers used in the present work were adapted from validated real-time RT-PCR assays developed in previous studies and extensively used for the diagnosis of NiV, MERS-CoV and REBOV infections (Mungall et al. 2006; Trombley et al. 2010; Corman et al. 2012). We optimized the triplex RT-PCR amplification conditions and triplex hapten-label combinations for the NALFIA device for the three selected targets. The gene targets for NiV, MERS-CoV and REBOV detection employed in our assay were nucleoprotein (*N*), upstream E (*UpE*) and matrix (*Vp40*), respectively, and the triplex NALFIA was standardized using IVT RNAs generated from clones of in-house designed synthetic DNA. This is the first report on a NALFIA-based molecular detection tool for NiV, MERS-CoV and REBOV. A schematic representation of the components of our triplex NALFIA is shown in Fig. 1. Our triplex one-step RT-PCR-based triplex NALFIA will be referred to as triplex NALFIA.

Results

Confirmation of the subcloned NiV *N*-pGEM-T Easy, REBOV *Vp40*-pGEM-T Easy and MERS-CoV *UpE*-pGEM-T Easy plasmids

After digestion of the NiV *N*-pGEM-T Easy plasmid with a size of 3115 bp by the *Pst* I enzyme, two fragments with sizes of 3037 bp and 78 bp were released, as *Pst* I cuts at positions 54/50 of the insert and 88/92 of the vector. Digestion of the REBOV *Vp40*-pGEM-T Easy plasmid by the *EcoR* I enzyme yielded a single linearized plasmid band of 3095 bp in size, as *EcoR* I cuts only the vector at a single site. Digestion of the subcloned MERS-CoV *UpE*-pGEM-T Easy plasmid by the *Ava* I enzyme gave a single linearized plasmid band of size 3107 bp, as *Ava* I cuts only the insert at 36/40 bp. The digestion pattern of the plasmids revealed that the target inserts were appropriately subcloned and inserted into the pGEM-T Easy vector.

Optimization of primer cocktail concentration and annealing temperature (*T*_a) for triplex amplification

The optimum equimolar composite concentration of the triplex primer cocktail for the NiV *N*, MERS-CoV *UpE* and REBOV *Vp40* targets was found to be 0.6 μM (Fig. 2A). There was a significant reduction in amplification at concentrations below 0.6 μM, while

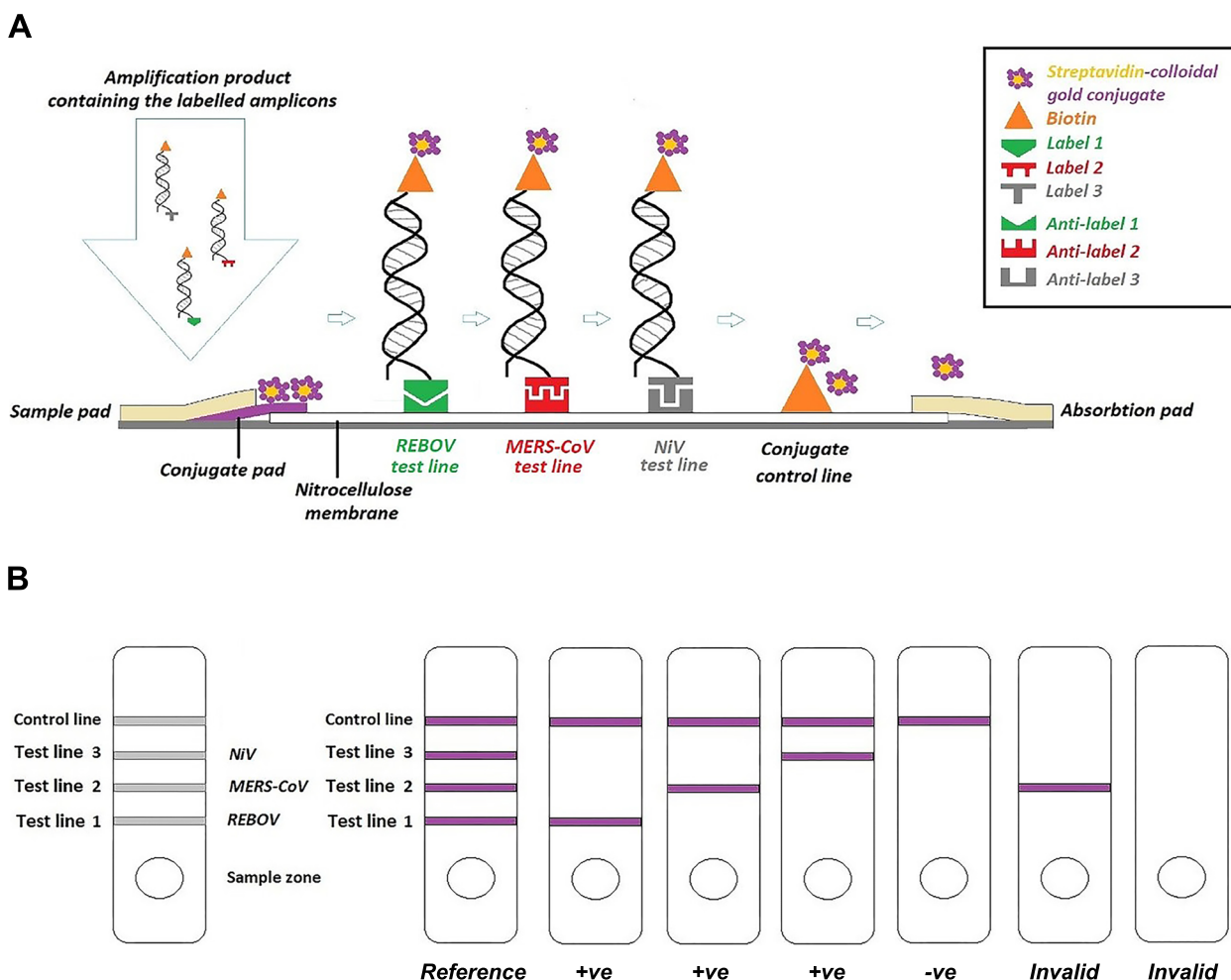


Fig. 1 **A** Schematic diagram of the triplex NALFIA. 5' labeled duplex target amplicons are generated by RT-PCR using forward and reverse primers with 5' tags. The labeled amplicons are then captured through the tags on the forward primer by the corresponding anti-tag/label antibody, which is the test line on the LFA device, while the biotin labeled on the reverse primer helps capture the detector system, i.e., the streptavidin-colloidal gold conjugate, and produces the signal on the test line in the presence of specific amplification. Label 1 - Alexa Fluor 488, Label 2 - Rhodamine Red, Label 3 - Digoxigenin. **B** Schematic diagram of the NALFIA triplex layout with coated lines, signal development and result interpretation. Signals at test line 1 and the control line indicate a positive test for REBOV and a negative test for NiV and MERS-CoV. Signals at test line 2 and the control line indicate a positive test for MERS-CoV and a negative test for REBOV and NiV. Signals at test line 3 and the control line indicate a positive test for NiV and negative tests for MERS-CoV and REBOV. No signal at the conjugate control line, regardless of signal development on any of the test lines, shows that the test is invalid

concentrations above 0.6 μ M resulted in dimers or excess primers. The amplification of NiV *N* and REBOV *Vp40* was evident till 150 nM, while the amplification of MERS-CoV *UpE* was evident till 100 nM composite concentration of primers in the triplex cocktail. The amplification was uniform for all three targets at all four tested annealing temperatures (Fig. 2B). The optimized annealing temperature of the triplex PCR was 60°C because the primer dimerisation was observed to have the least or no effect at 60°C.

In vitro transcription and confirmation

In vitro transcription yielded NiV *N*, MERS-CoV *UpE* and REBOV *Vp40* RNA transcripts of approximately 166 nt, 158 nt and 146 nt, respectively. PCR of NiV *N*, MERS-CoV *UpE* and REBOV *Vp40* resulted in no amplification, indicating the absence of carryover DNA in the IVT product. One-step RT-PCR of IVT RNA yielded specific amplicons indicating amplification exclusively from the IVT RNA template.

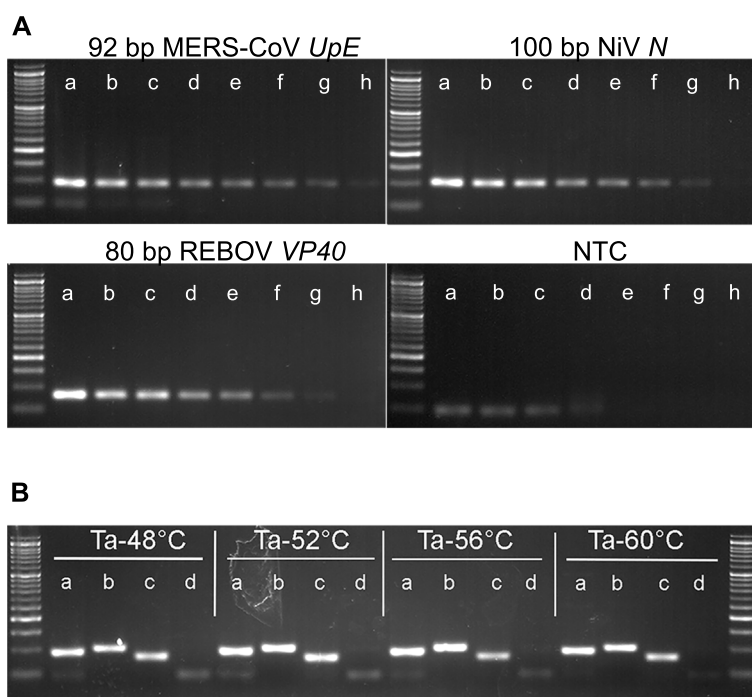


Fig. 2 **A** Optimization of the triplex primer concentration for amplification. PCR amplification was performed using different concentrations of a triplex primer cocktail composed of forward and reverse primer sets for MERS-CoV, NiV and REBOV in equimolar ratios. Lane a - 1.2 μ M, Lane b - 0.8 μ M, Lane c - 0.6 μ M, Lane d - 0.4 μ M, Lane e - 0.3 μ M, Lane f - 200 nM, Lane g - 150 nM, Lane h - 100 nM. Ladder - 50 bp. **B** Optimization of the annealing temperature for amplification. PCR optimization using different annealing temperatures for triplex amplification with the optimized triplex primer cocktail. Lane a - MERS-CoV (92 bp), lane b - NiV (100 bp), lane c - REBOV (80 bp), and lane d - NTC. Ladder - 50 bp

Optimization of the hapten labels and antibodies for the NALFIA device

The hapten labels DIG, fluorescein, Texas Red, Alexa Fluor 488 and rhodamine Red were reacted with their corresponding immobilized antibodies on nitrocellulose lateral flow strips. The hapten label DNP did not show any working signal with its corresponding immobilized antibody line on the lateral flow strip. There was nonspecific capture of the DIG label by the immobilized polyclonal anti-fluorescein and polyclonal anti-Texas Red antibody lines. Nonspecific capture of DIG by a

polyclonal anti-fluorescein antibody was not observed when the polyclonal anti-fluorescein antibody was replaced with a monoclonal anti-fluorescein antibody. There was cross-reactivity between the rhodamine red and texas red labels and their corresponding antibodies. The reactivities of the labels to their corresponding antibodies and the nonspecific and cross-reactivities for multiplexing compatibility are summarized in Table 1. Of the six hapten-label combinations, the finalized 5' labels on the forward primers NiV *N*, MERS-CoV *UpE* and REBOV *Vp40* for triplex NALFIA were digoxigenin,

Table 1 Summary of reactivity and compatibility evaluation of hapten label and antibody combinations for multiplexing on NALFIA device

	DNP	DIG	Fluorescein	Texas red	Alexa fluor 488	Rhodamine red
Polyclonal anti-DNP ab	Not reactive	Not reactive	Not reactive	Not reactive	Not reactive	Not reactive
Polyclonal anti-DIG ab	Not reactive	Reactive	Not reactive	Not reactive	Not reactive	Not reactive
Polyclonal anti-fluorescein ab	Not reactive	Nonspecific reaction	Reactive	Not reactive	Not reactive	Not reactive
Monoclonal anti-fluorescein ab	Not reactive	Not reactive	Reactive	Not reactive	Not reactive	Not reactive
Polyclonal anti-texas red ab	Not reactive	Nonspecific reaction	Not reactive	Reactive	Not reactive	Cross-reactive
Polyclonal anti-alexafluor 488 ab	Not reactive	Not reactive	Not reactive	Not reactive	Reactive	Not reactive
Polyclonal anti-tetramethyl rhodamine ab	Not reactive	Not reactive	Not reactive	Cross-reactive	Not reactive	Reactive

DNP Dinitrophenyl, DIG Digoxigenin, ab Antibody

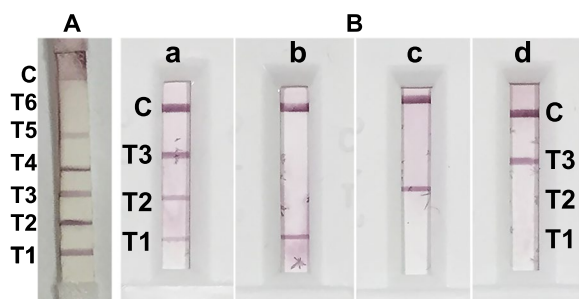


Fig. 3 Optimization of 5' primer label/tag and antibody combinations for NALFIA. **A** Hexaplex format; T6 - Dinitrophenyl (DNP), T5 - Digoxigenin (DIG), T4 - Fluorescein, T3 - Texas red, T2 - Alexa fluor 488, T1 - Rhodamine. Of the 6 label and antibody combinations tested, DNP and anti-DNP showed no reactivity, while the Texas Red antibody showed cross-reactivity with multiple labels. **B** Triplex format; three labels, DIG (T3), rhodamine red (T2) and Alexa fluor 488 (T1), were finally selected, and all further experiments were conducted using this combination

rhodamine red and Alexa Fluor 488, respectively. Signal development in the hexaplex and triplex formats is shown in Fig. 3.

Sensitivity of the NALFIA device for labeled PCR amplicons

Two microliters of undiluted labeled PCR product and its log dilutions was tested on the NALFIA device, and the band intensity in the NALFIA device decreased with increasing dilution for all three targets analyzed, which corresponded to the 3% agarose gel band gradation of 5 μ L PCR product (Fig. 4).

Limit of detection (LOD) of the Triplex NALFIA

The lowest copy numbers of IVT RNA detected by triplex NALFIA with 2 μ L of triplex RT-PCR products in a 13 μ L reaction were 8.21×10^4 for the NiV *N* target, 7.09×10^1 for the MERS-CoV *UpE* target, and 1.83×10^4 for the REBOV *Vp40* target (Fig. 5). Three percent agarose gel electrophoresis revealed that the RT-PCR amplification decreased linearly with increasing IVT RNA dilution for all three targets analyzed (data not shown, available in Additional file 1).

Specificity of the Triplex NALFIA

The band corresponding to the specific target was developed on the triplexed NALFIA device, and no cross-amplification or cross-reactivity was observed between the three targets (Figs. 5 and 6). Clinical samples positive for *Flaviviridae* (Japanese encephalitis virus, JEV; classical swine fever virus, CSFV), *Paramyxoviridae* (new castle disease virus, NDV), *Coronaviridae* (Infectious bronchitis virus, IBV), *Orthomyxoviridae* (Avian influenza virus, AIV), and *Picornaviridae* (Foot and mouth

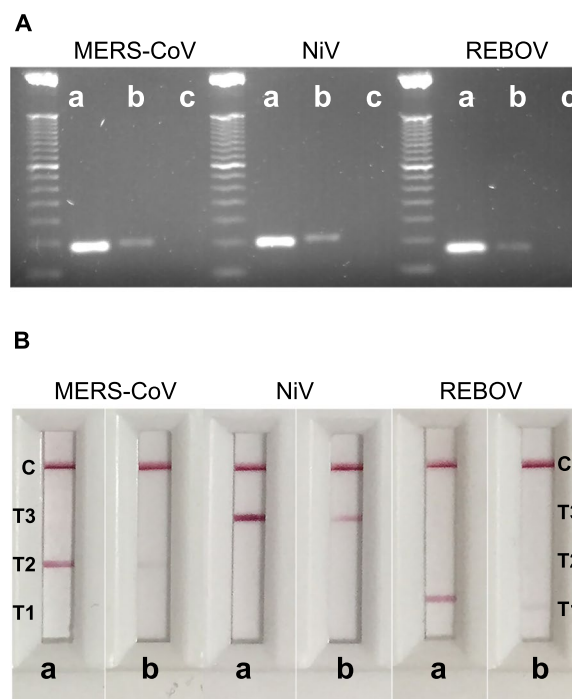


Fig. 4 Sensitivity of the NALFIA device for labeled PCR amplicons. **A** Band intensity of 5 μ L PCR product on a 3% agarose gel; lane a - undiluted PCR product, lane b - 1e-1 dilution, lane c - 1e-2 dilution, Ladder - 50 bp. **B** Band intensity of 2 μ L PCR product on the NALFIA device; lane a - undiluted PCR product, lane b - 1e-1 dilution

disease virus, FMDV)), *Arteriviridae* (porcine reproductive and respiratory syndrome virus, PRRSV), *Herpesviridae* (duck plague virus, DPV), and *Poxviridae* (swine pox virus, SPV) did not develop any visible signals on the bands designated for NiV, MERS-CoV or REBOV (Fig. 6).

Evaluation of Triplex NALFIA with simulated samples

Eleven NiV *N* IVT RNA-spiked samples and 15 non-spiked samples, 12 MERS-CoV *UpE* IVT RNA-spiked samples and 18 nonspiked samples and 10 REBOV *Vp40* IVT RNA-spiked samples and 14 nonspiked samples verified by TaqMan RT-qPCR were tested by triplex NALFIA. Ten out of 11 NiV IVT RNA-positive samples were found to be positive by triplex NALFIA, while 14 out of 15 negative samples were found to be negative by triplex NALFIA. All 12 MERS-CoV IVT RNA-positive samples were found to be positive by triplex NALFIA, and all 18 negative samples were found to be negative by triplex NALFIA. All 10 REBOV IVT RNA-positive samples were found to be positive by triplex NALFIA, and all 14 negative samples were found to be negative by triplex NALFIA. Additionally, no cross-reactivity was observed between the targets. The sensitivity and positive predictive value were 91% for the NiV *N* target and 100% for both the MERS-CoV *UpE* and REBOV *Vp40* targets.

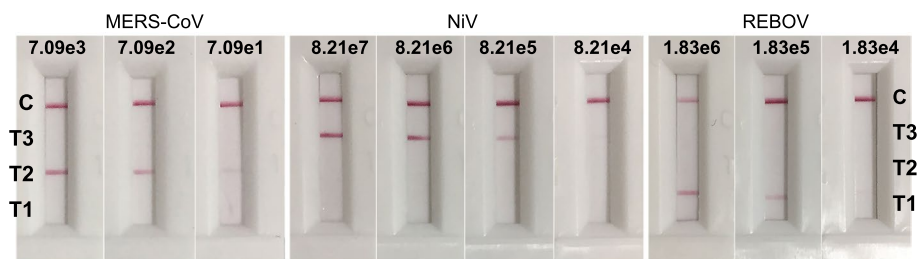


Fig. 5 Analytical sensitivity of the triplex-NALFIA. The lowest IVT RNA copy numbers were 7.09e1 for the MERS-CoV *UpE* target, 8.21e4 for the NiV *N* target and 1.83e4 for the REBOV *Vp40* target. Agarose gel electrophoresis (3%) of 5 μ L PCR product containing the labeled amplicons that correspond to this figure is available in Additional file 1

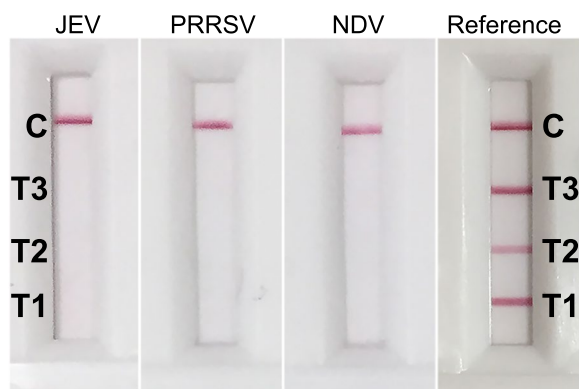


Fig. 6 Triplex NALFIA negative for JEV, PRRSV and NDV. JEV, Japanese encephalitis virus; PRRSV, porcine reproductive and respiratory syndrome virus; NDV, new castle disease virus

The specificity and negative predictive value were 93.3% for the NiV *N* target and 100% for both the MERS-CoV *UpE* and REBOV *Vp40* targets. The overall sensitivity and specificity of the triplex NALFIA were 96% and 97%, respectively. The compliance rate between triplex NALFIA and real-time RT-PCR was 92% for the NiV *N* target and 100% for the MERS-CoV *UpE* and REBOV *Vp40* targets.

Repeatability

Triplex NALFIA, which was conducted three times on two simulated positive samples of each of the three targets, yielded consistent positive results, indicating 100% repeatability of the assay.

Discussion

In human outbreaks of Nipah virus (NiV), Middle East respiratory syndrome coronavirus (MERS-CoV), and ebolavirus, bats have been directly or indirectly implicated with or without the involvement of an intermediate host (Leroy et al. 2005; Jayme et al. 2015; Halpin et al. 2011; Ithete et al. 2013; Annan et al. 2013). To determine

the prevalence of these viruses in bats and other hosts and reservoirs, continuous monitoring and swift implementation of prevention and control policies and rapid and user-friendly diagnostics of these viruses are needed. Assays available for virus detection and diagnosis mostly require centralized facilities and sophisticated operation, which renders them unsuitable for routine screening in remote and low-resource settings. Our work was conceptualized based on the need for and benefits of a multiplexed assay in our region where multiple NiV outbreaks in humans have been reported with evidence of prevalence in bats (Epstein et al. 2008; Yadav et al. 2012, 2018, 2019) alongside threats from the introduction of MERS-CoV and REBOV from neighboring countries. The triplex NALFIA, although intended for bats, can also be used for screening other hosts of these viruses because it detects virus genomes irrespective of the host. Multiplexing saves time and allows testing with limited sample quantity; thus, it is suitable in low-resource settings for simultaneous three-virus surveillance and first-line screening of NiV, MERS-CoV and REBOV infections in bats and other hosts. The main concern of a multiplex assay is potential cross-reactivity, which limits the number and types of biomarkers that can be combined. Previous studies have reported the careful selection of primers and optimization of hapten-label combinations for successful multiplexing in amplification-based NALFIA for other pathogens (Crannell et al. 2016; Mens et al. 2012a; Kamphee et al. 2015; Blažková et al. 2009). The current assay reports the use of triplex one-step RT-PCR amplification with labeled forward and reverse primers and the visual detection of specific PCR amplicons on a triplexed NALFIA device. Multiplexed NALFIA devices with PCR-based amplification using labeled forward and reverse primers have been reported to have high analytical sensitivity and specificity in a previous study for the detection of *Plasmodium* DNA (Mens et al. 2012b). In another study of multiplexed NALFIA for DNA detection and differentiation of three diarrheal protozoa, a labeled probe,

a labeled primer, and an unlabeled primer were employed for isothermal amplification (Crannell et al. 2016).

The sensitivity of the present NALFIA device for end point detection of the triplex RT-PCR product was compared with that of agarose gel electrophoresis and was found to correspond to the sensitivity of agarose gel electrophoresis, which indicates that NALFIA is a rapid alternative to agarose gels. The analytical sensitivity of the NALFIA device was reported to be 10-fold greater than the analytical sensitivity of agarose gel electrophoresis in a previous report (Blažková et al. 2009). The use of the NALFIA device as a naked eye endpoint detection method not only overcomes the complexity of conventional post-amplification steps but also introduces the scope of point-of-care in the nucleic acid amplification-based diagnosis of infectious diseases. It is evident from previous reports on the detection of other organisms that isothermal amplification-backed NALFIA is a good option for POCD (Crannell et al. 2016; James et al. 2010; Krölov et al. 2014). Recently, LAMP and other isothermal assay-based multiplex NALFIAs have been successfully developed for the detection of multiple gene targets of SARS-CoV-2, demonstrating the feasibility of multiplexed NALFIA (Zhu et al. 2020; Zhang et al. 2021; Jia et al. 2021).

The sequences of the primers used in the present study have been validated in previous real-time RT-PCR assays. This circumvents the need for essential validation in different organisms. Adaptation of published primers in other assays has been reported (Zhang et al. 2016). We analyzed the cross-amplification at the RT-PCR level and cross-reactivity at the endpoint of the NALFIA device. Amplification was specific for the respective selected targets, and no cross amplification was observed. At the level of the NALFIA device, six combinations of labels and antibodies were initially tested for specific reactivity and compatibility in multiplexing. Haptens for 5' end labeling of forward oligos were dinitrophenyl (DNP), digoxigenin (DIG), Texas Red, fluorescein, rhodamine Red and Alexa Fluor 488. The following antibodies were used: polyclonal anti-DNP, polyclonal anti-DIG, polyclonal anti-Texas Red, polyclonal anti-fluorescein, monoclonal anti-fluorescein, polyclonal anti-tetramethylrhodamine, and polyclonal anti-Alexa Fluor 488. Among the six tested signals, there was no working signal at the DNP test line. The failure of DNP to interact with its antibody could be due to various factors, such as steric hindrance, low sensitivity of the antibody, batch and lot defects, etc. Further testing of the combination by changing the brand and the lot of both DNP and its antibody could be successful, as successful use of DNP has already been reported in a previous assay (Mens et al. 2012a). However, due to time constraints, the DNP combination

was not tested further and was excluded from subsequent assays. There was cross-reactivity between Texas red and rhodamine red, which could be due to the structural relatedness between the two compounds. Although Texas Red and DIG are unrelated haptens, the polyclonal anti-Texas Red antibody reacted nonspecifically with the DIG label. The DIG label was also found to react nonspecifically with the polyclonal anti-fluorescein antibody, but this problem was solved when the polyclonal antibody was replaced with a monoclonal antibody. Similarly, the problem of nonspecific reactivity observed with the anti-Texas Red antibody with the DIG label could also be solved by using a monoclonal antibody; however, this experiment was not performed due to the high cost of the monoclonal antibody.

The three final label-antibody combinations selected for our triplex-NALFIA were DIG, rhodamine red, Alexa Fluor 488 and their corresponding antibodies mentioned above. Alexa Fluor 488 and rhodamine red have already been successfully employed in a previous study of a prototype multiplex NALFIA (Crannell et al. 2016). DIG has been used as a standard label in most multiplex and duplex NALF assays (Mens et al. 2012a; Kamphée et al. 2015; Posthuma-Trumpie et al. 2009). The methods used for testing other label antibody combinations have also been discussed briefly in a previous study (Crannell et al. 2016). The three final label-antibody combinations selected in the present study were not cross-reactive. However, for the three label-antibody combinations, the sensitivity of the combination of rhodamine red and anti-tetramethyl rhodamine antibody was slightly lower than that of the other two, as revealed by the weaker signal at the MERS-CoV test line on the NALFIA device despite the amplification product having a band intensity similar to that of the other two targets. The readings were recorded within a maximum time of 15 min, and the appearance of nonspecific and ghost bands observed beyond this period was ignored. Most reported NALFIAs are monoplexes or duplexes, and reports on multiplex NALFIAs are limited. Therefore, the present work is an attempt to demonstrate the compatibility of tags in a multiplex setup that is otherwise successfully employed in a monoplex setup. The limitation of such an assay, wherein endpoint detection on an LFA strip is based on the capture of a labeled amplicon DNA duplex, is that there is a risk of false positive signal development at the endpoint due to dimerization of primers during amplification. However, we performed amplification at an annealing temperature of 60°C, and no significant dimerization was observed in the agarose gels; therefore, dimerization was not detectable at the endpoint of the lateral flow strip. On using nonspiked negative biological samples, out of the three primer sets, the

Nipah virus primer set displayed a tendency to develop dimers, which were seen as faint bands on the LFA strip, but this signal developed well beyond our maximum reading point and hence was ignored. We believe these dimerization reactions are influenced by the PCR master mix and the period between template addition and the start of thermal cycling. Using stringent hot-start master mixes, reducing the time between template addition and the start of amplification, among other good practices, may help reduce the scope of primer dimerization. Our hapten label streamlining strategy is novel, although it is slightly similar to previous work by Crannel and his team (Crannell et al. 2016), and the current assay was conceptualized independently, as a previous report was not published at the time of development of the current assay. The label and antibody combination highlighted in the current work can be applied to the detection of other pathogens if the primers are replaced with specific primers corresponding to the desired targets.

The test control included in our triplex NALFIA was the BSA-biotin conjugate line for the LFA part. Including an internal control (IC) for PCR amplification may improve the quality of the overall assay; however, in our case, the inclusion of IC meant adding a fourth test line on the triplex LFA strip and replacing one of the targets in our hexaplex layout with IC. Although we successfully attempted a hexaplex layout with other targets, the efficiency of such high multiplexing was not fully determined, nor were reports available. It is expected that the multiplexing efficiency will decrease with more test lines; therefore, we limited the test lines to triplex only for the specific targets aside from the conjugate control line. This reduced efficiency of high multiplexing in endpoint LFA readouts may be overcome by adopting a different strategy for coating capture proteins on the membrane (Anfossi et al. 2018). Amplification multiplexing of more than three targets has been successfully deployed in real-time PCR using specific labeled probes; however, conventional PCR multiplexing beyond four targets is not as efficient (Shaopeng et al. 2023). These points may be held accountable for triplexed DNA amplification-based LFA end-point detection assays that have been developed without IC in previous studies (Crannell et al. 2016). Nevertheless, every batch of tests needs to have known positive and negative control runs.

We suspect that one probable reason for the unusually high LOD for the NiV target was the low concentration of the primers of NiV *N* target in the triplex amplification. We also maintained an equimolar ratio of the triplex primer cocktail for uniformity and reducing the scope of dimerization; however, the low sensitivity of the NiV *N* target could have been circumvented by using a triplex cocktail primer ratio of 2:1:1 or 3:1:1 (NiV *N*: *REBOV*

Vp40: *MERS-CoV N*). The triplex NALFIA was evaluated on negative samples positive for other viruses and showed no signal, which indicates the specificity of the assay for its intended targets. Additionally, dimers that could have been generated during amplification did not produce visible signals on the NALFIA device. Due to the unavailability of clinically positive samples at the time of development of the current assay, a simulation of positive samples was created by spiking samples composed of sera, swabs, tissues and blood from apparently healthy bats, pigs and camels with IVT RNAs from the respective targets, and the spiked samples were then used for evaluating the triplex NALFIA. Despite the same IVT RNA spiking concentration used, the positive response signal by triplex NALFIA varied from sample to sample, which could be due to differences in the final IVT RNA concentration post extraction. In our study, we used TRIzol and TRIzol LS reagent for the extraction of RNA from negative and simulated positive samples, as our specimens also included tissues. Most specimens presented for screening or diagnosis are oropharyngeal swabs, serum or blood, from which viral RNA may be extracted by safer and more common methods, i.e., silica membrane spin columns or magnetic bead-based extraction methods. Although postmortem tissue specimens require additional processing and the use of stronger and more hazardous lysis buffers, they are mostly sent to and processed at central laboratories where appropriate safety measures and hazard management procedures are in place. However, we have not tested the LOD based on different RNA extraction methods, and comparing different RNA extraction methods appropriate for specimen type may improve the assessment/interpretation of the assay performance. Nevertheless, there is a need for further evaluation of the operating range of the triplex NALFIA using quantitated virus, individually for each virus target within the corresponding sample matrix—spiked or clinical specimen. However, this can only be performed at a BSL4 containment facility.

Although the work in our article was performed before the COVID-19 pandemic, the pandemic has presented challenges pertaining to timely diagnosis and surveillance of novel, emerging/re-emerging and exotic viral infections, which has re-enforced our objective to develop such an assay. Important challenges pertaining to virus detection observed during the COVID-19 pandemic include the need for immediate diagnosis as well as extensive surveillance in the human population irrespective of the resource setting; the need for surveillance in susceptible animals and reservoir population for identifying risk factors and subsequent mitigation programmes; the multistep complexity of the molecular diagnostic procedure and the need for compliance with biosafety

and PCR workflows limiting the operation only within centralized laboratory buildings; the shortage of kit supplies; and sample deterioration due to logistical issues. Some of the solutions to these challenges include the decentralization of laboratory diagnosis, the availability of portable molecular test setups for wider distribution to cover resource-limited areas, the design of energy-autonomous itinerant POCs, the consolidation of multistep procedures, e.g., nucleic acid amplification tests using clinical specimens, sans the nucleic acid purification step, and the simplification of existing technologies for easy immediate development and implementation. Our strategy was to test and apply validated reference primers for RT-qPCR diagnosis to conventional multiplexed amplification and end-point detection by LFA as a proof-of-concept test. Such simplification cannot replace the gold standard role that RT-qPCR plays; however, the aim was to attain a more widely distributable testing platform at times of need. POC models with itinerant and stationary options have been designed and developed for LAMP-based detection of SARS-CoV-2, which is energetically autonomous and features three discriminating but retractable areas for sample processing, master mix preparation and amplification (Alva-Araujo et al. 2021). Extraction-free approaches leading to the consolidation of testing procedures increasingly seem to be a viable option. Clinical or field specimens such as respiratory secretions and serum are commonly targeted for most viral nucleic acid detection for diagnosis or surveillance. Such specimens are less complex than tissues, stool/feces and soil and can be optimized for direct amplification of viral nucleic acid without going through viral RNA/DNA purification; for example, several methods have been proposed and tested for SARS-CoV-2 RNA detection without the viral RNA purification step (Smyrlaki et al. 2020; Castellanos-Gonzalez et al. 2021), while many commercially available inhibitor-resistant standard PCR reagents have been evaluated for direct amplification of nucleic acid from other pathogens (Hall et al. 2013). We believe our assay format can be amalgamated with some of the

POC features described above to widen its scope of application at remote locations and in low-resource settings.

Conclusion

Emerging infectious diseases (EIDs) are a significant threat to global public health, and bats are increasingly implicated in viral EID events by serving as reservoir hosts for viruses that can opportunistically cross species barriers to infect humans and other domestic as well as wild mammals. We developed a triplex one-step RT-PCR-based nucleic acid lateral flow immunoassay (NALFIA) for simultaneous detection of NiV, MERS-CoV and REBOV RNA targets using primers labeled with different haptens and antibodies specific to the haptens. This assay is mainly intended for screening bats but can also be applied to other reservoirs and susceptible hosts of these three viruses.

Methods

Primer sequences for NiV, MERS-CoV and REBOV

The nucleoprotein (*N*) gene of NiV, upstream E (*UpE*) gene of MERS-CoV and matrix (*Vp40*) gene of REBOV were selected as targets for detection because these genes are sensitive diagnostic markers. Based on the diagnostic recommendations of the WHO and WOA, forward and reverse primers targeting these genes were selected from published literature, as listed in Table 2.

Template design and IVT RNA preparation

The nucleotide sequences of the PCR targets of NiV *N* (100 bp), MERS-CoV *UpE* (92 bp) and REBOV *Vp40* (80 bp) were downloaded from the NCBI GenBank and constructed in silico in tandem using EditSeq of DNASTAR Lasergene software. These selected gene target regions are highly conserved, and the details of the sequence alignment results can be found in Additional file 2. The pBluescript II SK (+) plasmid containing the target construct was synthesized by GenScript (USA) (Fig. 7).

Table 2 Details of primers used in the development of triplex NALFIA

Virus	Target gene	Primer		Amplicon length (bp)	Ta	Reference
		Sequence 5'-3'	Length			
NiV	<i>N</i>	F	TCAGCAGGAAGGCAAGAGAGTAA	23	60 °C	Mungall et al. 2006
		R	CCCCTTCATCGATATCTTGATCA	23		
REBOV	<i>Vp40</i>	F	CTATGGTTATCACCCAGGATTGTG	24	60 °C	Trombley et al. 2010
		R	GTAACCTATCCTGCTTGCCATGTG	24		
MERS-CoV	<i>UpE</i>	F	GCAACGCGGATTCAAGTT	18	58 °C	Corman et al. 2012
		R	GCCTCTACACGGGACCCATA	20		

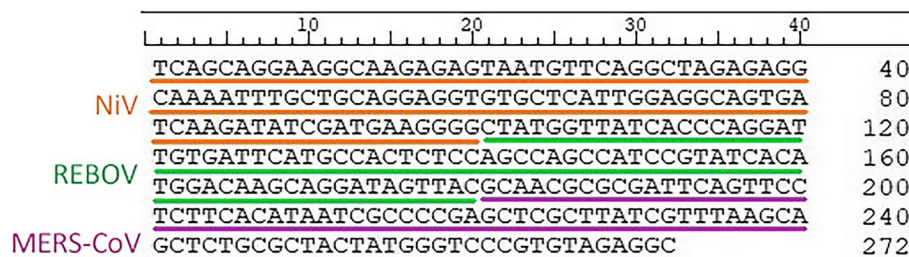


Fig. 7 A 272 bp gene construct composed of NiV *N* (100 bp), REBOV *Vp40* (80 bp) and MERS-CoV *UpE* (92 bp) synthesized in tandem at the EcoRI site in the pBluescript II SK (+) vector (vector sequence is not included in the figure). The NCBI GenBank accession numbers of the sources of the target genes are EU620498.1 (NiV), AB050936.1 (REBOV), and JX869059.2 (MERS-CoV). These selected gene target regions are highly conserved, and the details of the sequence alignment results can be found in Additional file 2

Since the fusion target DNA construct may generate multiple nonspecific amplicons when used as a template with a triplex primer cocktail owing to multiple combinations of forward and reverse primer binding sites present in tandem, it was necessary to separate the targets from the fused construct to make them functional as discrete templates for the triplex primer cocktail. Therefore, individual target sequences were PCR amplified, and the amplicons were subcloned and inserted into separate pGEM-T Easy vectors (Promega) at the TA cloning site. The resulting clones were then confirmed by restriction enzyme digestion: NiV *N*-pGEM-T Easy plasmid by *Pst* I, the REBOV *Vp40*-pGEM-T Easy plasmid by *Eco*R I and the MERS-CoV *UpE*-pGEM-T Easy plasmid by *Ava* I.

For in vitro transcription, the subcloned plasmids NiV *N*-pGEM-T Easy, REBOV *Vp40*-pGEM-T Easy and MERS-CoV *UpE*-pGEM-T Easy were first linearized by the *Sal* I enzyme (Promega) to create a 5' overhang. RNA from the NiV *N*, REBOV *Vp40* and MERS-CoV *UpE* targets was transcribed from 600 ng of linearized and purified plasmids using a TranscriptAid T7 High Yield Transcription Kit (Thermo Scientific). The IVT master mix was used according to the manufacturer's instructions, and the reaction was performed at 37°C for 6–7 h. The estimated transcript lengths were 166 nt for NiV, 146 nt for REBOV and 158 nt for MERS-CoV. The IVT products were treated with 3 U of Turbo DNase I enzyme (Ambion) and purified 2–3 times with TRIzol LS (Ambion) to completely remove the carry-over plasmid DNA template. The IVT RNAs were quantitated by a Qubit fluorometer using Quant-it RNA BR reagent (Molecular Probes) and stored at -80°C in small aliquots until further use. The RNA copy number was calculated using the online software NEBioCalculator from New England Biolabs (<https://nebiocalculator.neb.com>) with the following formula: RNA copy number = moles of RNA $\times 6.022 \times 10^{23}$ (Fajardo et al. 2017).

Optimization of triplex amplification conditions

A triplex primer stock cocktail was prepared by mixing the NiV *N*, MERS-CoV *UpE* and REBOV *Vp40* specific forward and reverse primers in equimolar ratios and was diluted in series to yield 8 different equimolar primer cocktails of 1.2 μ M, 0.8 μ M, 0.6 μ M, 0.4 μ M, 0.3 μ M, 0.2 μ M, 0.15 μ M and 0.1 μ M composite concentrations. Each cocktail concentration was subjected to PCR amplification of individual subcloned DNA target plasmid templates, 10.5 pg of NiV *N*-pGEM-T Easy, 127 pg of REBOV *Vp40*-pGEM-T Easy and 7.7 pg of MERS-CoV *UpE*-pGEM-T Easy using 2X Verso hot-start PCR buffer (Thermo Scientific). The reaction was set up in a 15 μ L final volume, and the thermal cycling conditions were as follows: hot-start and initial denaturation at 95°C for 15 min, 35 cycles of denaturation at 95°C for 15 s, annealing at 58°C (MERS-CoV target) and 60°C (NiV and REBOV targets) for 30 s and extension at 72°C for 15 s, followed by a final extension at 72°C for 5 min and holding at 4°C. Using the final optimum composite primer concentration of 0.6 μ M, the annealing temperature of the triplex amplification was optimized by testing four different temperatures—48°C, 52°C, 56°C and 60°C—in a thermal cycler with Veriflex block (ABI Veriti 96-Well Fast Thermal Cycler, Thermo Fisher). The reaction was set up in a 15 μ L final volume, and the thermal cycling conditions were as follows: hot-start and initial denaturation at 95°C for 15 min; 35 cycles of denaturation at 95°C for 15 s; annealing at 48°C, 52°C, 54°C and 60°C for 30 s; and extension at 72°C for 15 s, followed by a final extension at 72°C for 5 min and a hold at 4°C. Triplex amplification was also observed for any nonspecific interactions among primers (homodimers and heterodimers) and between primers and nonself templates.

Confirmation of IVT RNA

The IVT RNAs of NiV, MERS-CoV and REBOV were diluted to 2×10^{-3} and confirmed by their respective monoplex one-step RT-PCR with specific primers using

the Verso 1-step RT-PCR kit (Thermo Scientific). The reaction was set up in a 10 μ L final volume with 100 nM each of the unlabeled forward and reverse primers for each target. The thermal cycling conditions were as follows: RT step at 50°C for 15 min, hot-start and initial denaturation at 95°C for 15 min, 35 cycles of denaturation at 95°C for 15 s, annealing at 60°C for 30 s and extension at 72°C for 15 s, followed by a final extension at 72°C for 5 min and holding at 4°C. IVT RNA products (2×10^{-3} dilution) were tested for the absence of a carry-over plasmid template by PCR using Taq 2X master mix (NEB). A negative PCR result confirmed the absence of a carryover plasmid in the IVT product.

Optimization of compatible combinations of hapten labels and antibodies for triplex NALFIA

For selective and specific detection of our targets, the forward primers were tagged at the 5' end with different hapten labels to be captured by their corresponding antibodies immobilized on a lateral flow nitrocellulose membrane. To generate a color signal, all reverse primers were tagged at the 5' end with biotin to bind with a streptavidin-colloidal gold conjugate. Different hapten labels were

initially tested with corresponding capture antibodies (Table 3) for sensitive and specific interactions between labels and capture antibodies in a preliminary batch of monoplex, duplex and triplex lateral flow nitrocellulose strips (data not shown). For further testing of label-antibody compatibility in multiplexing, hexaplex lateral flow nitrocellulose strips were also fabricated and tested with PCR-labeled amplicons. Among the six label-antibody combinations tested, the three best combinations were selected, and our final triplexed NALFIA device was fabricated. The order of the antibody test lines and control lines in the hexaplex and triplex formats of the lateral flow strips are displayed in Table 4.

Nucleic acid lateral flow immunoassay (NALFIA) device

NALFIA devices with three test lines and a control line were custom manufactured at Ubio Biotechnology Pvt. Ltd., Cochin, (India) *via* a batch method. Three consecutive test lines of 0.11 μ L/mm of each capture antibody with a width of 0.5 mm were applied at a rate of 0.11 μ L/mm at a concentration of 1 mg/mL in coating buffer on a nitrocellulose membrane with a 0.47 mm thickness and a 0.22 μ m pore size. Biotin-BSA was applied as the

Table 3 Hapten labels for 5' end-labeling of forward and reverse primers and their corresponding antibodies

Combination	5' hapten label on forward primer	Antibody against 5' label on forward primer	5' hapten label on reverse primer
1	Dinitrophenyl (DNP), IDT	Polyclonal anti-DNP ab, molecular probe	Biotin, Eurofins
2	Digoxigenin (DIG), Eurofins	Polyclonal anti-DIG ab, pierce	Biotin, Eurofins
3	Texas Red, Eurofins	Polyclonal anti-texas red ab, molecular probe	Biotin, Eurofins
4	Fluorescein, Eurofins	Polyclonal anti-fluorescein ab, molecular probe and monoclonal anti-fluorescein ab, molecular probe	Biotin, Eurofins
5	Rhodamine Red, Eurofins, IDT	Polyclonal anti-tetramethyl rhodamine ab, molecular probe	Biotin, Eurofins
6	Alexa fluor 488, Eurofins	Polyclonal anti-alexafluor 488 ab, molecular probe	Biotin, Eurofins

ab Antibody

Table 4 Layout of hexaplex and triplex NALFIA strips with specific order of the label antibodies as test lines

Hexaplex		Triplex	
	<i>Absorbtion Pad</i>	<i>Absorbtion pad</i>	
Control line	Conjugate control	Conjugate control	Control line
Test line 1	Anti-DNP ab	Anti-DIG ab	Test line 1
Test line 2	Anti-DIG ab	Anti- Rhodamine ab	Test line 2
Test line 3	Anti-Fluorescein ab	Anti-Alexa Fluor 488 ab	Test line 3
Test line 4	Anti-Texas Red ab	<i>Sample pad/Conjugate pad</i>	
Test line 5	Anti-Alexa fluor 488 ab		
Test line 6	Anti-Rhodamine ab		
	<i>Sample pad/Conjugate pad</i>		

DNP Dinitrophenyl, DIG Digoxigenin, ab Antibody

conjugate control at a width of 0.5 mm at 0.75 mg/mL. A conjugate pad made of 5 mm wide glass fibers was impregnated with a streptavidin-colloidal gold conjugate (10 µg/mL) by soaking in a 1:2 dilution of conjugate solution, which was prepared at a 1:1 ratio in conjugation buffer. The sample pad consisted of 18 mm wide glass fibers, while the absorption pad consisted of 20 mm long cellulose fibers. Individual 3.2 mm wide strips were cut after manual lamination of the components followed by manual housing (6.9 cm × 2 cm polypropylene, TV Plastics). All handling was performed at ≤ 10% humidity and 30°C room temperature. A schematic representation of the NALFIA device with interpretation is shown in Fig. 1.

Sensitivity of the NALFIA device for labeled PCR amplicons

Two microliters of undiluted labeled monoplex PCR products of each target and their log dilutions were added to the sample pads of the NALFIA devices. Migration buffer (10 mM PBS, 1% BSA, 0.05% Tween 20, pH 7.5) was added dropwise after the PCR products were added until the conjugate front disappeared. The band intensity in each device was subsequently observed within a signal development period of up to 15 min. The bands on the devices were compared with the corresponding band gradation in 3% AGE for each target of a 5 µL load volume.

Determination of the limit of detection (LOD) of the Triplex NALFIA

Ten-point serial log dilutions (10^{-1} to 10^{-10}) of the quantitated stock IVT RNA templates of the NiV, MERS-CoV, and REBOV targets were prepared, and each dilution of the three targets was subjected to amplification by triplex one-step RT-PCR. Using a Verso 1-Step RT-PCR kit (Thermo Scientific), reactions with a final volume of

13 µL were performed using 0.6 µM triplex primer cocktail in an equimolar ratio of labeled forward and reverse primers for each target. The linearity of the amplification was visualized using 5 µL products in 3% agarose gel in 1 × TAE buffer, and the sensitivity or the limit of detection of the triplex NALFIA was evaluated using 2 µL of the product on the NALFIA device.

Specificity of the triplex NALFIA

The specificity of triplex NALFIA was evaluated by observing any nonspecific signals arising from interactions among the primers in the triplex cocktail and between the triplex primers and the templates. The specificity of the triplex NALFIA was also analyzed by testing clinical samples negative for NiV, MERS-CoV and REBOV but positive for *Flaviviridae* (JEV and classical swine fever virus, CSFV), *Paramyxoviridae* (NDV), *Coronaviridae* (infectious bronchitis virus, IBV), *Orthomyxoviridae* (avian influenza virus, AIV), *Picornaviridae* (foot and mouth disease virus, FMDV), *Herpesviridae* (uck DPV), *Arteriviridae* (PRRSV), and *Poxviridae* (suipox virus, SPV).

Evaluation of triplex NALFIA with samples spiked with IVT RNA and nonspiked samples

For the simulation of positive samples, an assorted group of samples comprising sera, oropharyngeal swabs, tissue and whole blood from bats (*Pteropus giganteus*), camels and pigs, which represent the target species and sample-source population of the three selected viruses, were spiked with 28 pg to 56 pg NiV N IVT RNA, 230 fg to 460 fg MERS-CoV *UpE* IVT RNA, and 5.5 pg to 11 pg REBOV *Vp40* IVT RNA at the lysis step of RNA extraction (Table 5). TaqMan RT-qPCR was performed to validate the samples. The nonspiked

Table 5 Simulated positive samples used for triplex NALFIA evaluation

Species	Sample type	IVT RNA	No. of Samples spiked	Amount of IVT RNA per extraction	RNA extraction by
Bat (<i>Pteropus</i>)	Oro-pharyngeal swab	NiV N	2	~28 pg	TRIzol LS
		REBOV <i>Vp40</i>	2	~5.5 pg	
		MERS <i>UpE</i>	3	~230 fg	
Pig		NiV N	2	~28 pg	
		REBOV <i>Vp40</i>	1	~5.5 pg	
Camel	Serum	MERS <i>UpE</i>	3	~230 fg	
Pig		NiV N	1	~28 pg	
		REBOV <i>Vp40</i>	1	~5.5 pg	
Camel	Tissue	MERS <i>UpE</i>	6	~460 fg	TRIzol
Pig		NiV N	3	~56 pg	
		REBOV <i>Vp40</i>	3	~11 pg	
Bat (<i>Pteropus</i>)	Whole blood	NiV N	3	~28 pg	
		REBOV <i>Vp40</i>	3	~5.5 pg	

and spiked samples were then subjected to amplification using the Verso 1-step RT-PCR kit (Thermo Scientific): the reaction was set up in 10 μ L final volumes with 600 nM of labeled triplex primer cocktail and 1–3 μ L of RNA template. The thermal cycling conditions were as follows: RT step at 50°C for 15 min, hot-start and initial denaturation at 95°C for 15 min, 35 cycles of denaturation at 95°C for 15 s, annealing at 60°C for 30 s and extension at 72°C for 15 s, followed by a final extension at 72°C for 5 min and holding at 4°C. For readout on the NALFIA device, 2 μ L of triplex RT-PCR product was loaded on the NALFIA device, and the results were read between 1–15 min. Using RT-qPCR as a standard test, the sensitivity, specificity and positive and negative predictive values (PPV and NPV) for the triplex NALFIA were calculated (Trevethan 2017).

Repeatability of the triplex NALFIA

Triplex-NALFIA was performed three times with two spiked samples for each virus target to demonstrate the repeatability of the assay.

Abbreviations

Ab	Antibody
AGE	Agarose gel electrophoresis
BSA	Bovine serum albumin
COVID-19	Coronavirus disease 2019
DIG	Digoxigenin
DNA	Deoxyribonucleic acid
DNP	Dinitrophenyl
EID	Emerging infectious disease
IVT	In vitro transcription
LAMP	Loop-mediated isothermal amplification
MERS-CoV	Middle East respiratory syndrome coronavirus
N	Nucleoprotein
NALFIA	Nucleic acid lateral flow immunoassay
NiV	Nipah virus
NPV	Negative predictive value
PBS	Phosphate-buffered saline
PCR	Polymerase chain reaction
POC	Point-of-care
PPV	Positive predictive value
REBOV	Reston ebolavirus
RNA	Ribonucleic acid
RT-PCR	Reverse transcription polymerase chain reaction
RT-qPCR	Reverse transcription quantitative polymerase chain reaction
SARS-CoV-2	Severe acute respiratory syndrome coronavirus 2
Ta	Annealing temperature
UpE	Upstream of the envelope protein-encoding gene
Vp	Viral protein
WHO	World Health Organization
WOAH	World Organization for Animal Health

Supplementary Information

The online version contains supplementary material available at <https://doi.org/10.1186/s44149-024-00127-w>.

- Supplementary Material 1.
- Supplementary Material 2.
- Supplementary Material 3.

Acknowledgements

We thank the Ubio Biotechnology Ltd, Kochi (India) for the fabrication of NALFIA device. We also thank the Director, ICAR-National Institute of High Security Animal Diseases (NIHSAD), Bhopal, India. Special thanks to Ms. Chitra for her help in IVT RNA quantitation and sample spiking.

Authors' contributions

AAR and SC conceptualized and designed the work; STS optimized the capture antibody coating on the NCM of the NALFIA device; SC reviewed the literature, optimized the methodology, performed the experiments, analyzed and interpreted the results, and prepared and revised the manuscript draft; AM and AAR reviewed and edited the manuscript draft; AM, AKP, DDK and VPS provided the resources and lab facility; DDK and AAR supervised the overall work.

Funding

This work was partially funded by the Department of Biotechnology, Ministry of Science and Technology, Government of India (DBT) under grant number ADMaC DBT-NER/LIVS/11/2012.

Availability of data and materials

All data generated or analyzed during this study are included in this published article.

Declarations

Ethics approval and consent to participate

Not applicable.

Consent for publication

Not applicable.

Competing interests

The authors declare that they have no competing interests.

Received: 29 February 2024 Accepted: 29 May 2024

Published online: 24 June 2024

References

- Alva-Araujo, J.P., O. Escalante-Maldonado, and R.A.C. Ramos. 2021. Design of a point-of-care facility for diagnosis of COVID-19 using an off-grid photovoltaic system. *Environment, Development and Sustainability* 23 (8): 11990–12005. <https://doi.org/10.1007/s10668-020-01153-7>.
- Anfossi, L., F. Di Nardo, S. Cavalera, C. Giovannoli, and C. Baggiani. 2018. Multiplex lateral flow immunoassay: an overview of strategies toward high-throughput point-of-need testing. *Biosensors (Basel)* 9 (1): 2. <https://doi.org/10.3390/bios9010002>.
- Annan, A., H.J. Baldwin, V.M. Corman, S.M. Klose, M. Owusu, E.E. Nkrumah, E.K. Badu, P. Anti, O. Agbenyega, B. Meyer, et al. 2013. Human betacoronavirus 2c EMC/2012-related viruses in bats, Ghana and Europe. *Emerging Infectious Diseases* 19: 456–459. <https://doi.org/10.3201/eid1903.121503>.
- Barrette, R.W., S.A. Metwally, J.M. Rowland, L. Xu, S.R. Zaki, S.T. Nichol, P.E. Rollin, J.S. Towner, W.J. Shieh, B. Batten, et al. 2009. Discovery of swine as a host for the Reston ebolavirus. *Science* 325: 204–206. <https://doi.org/10.1126/science.1172705>.
- Blažková, M., M. Koets, J.H. Wichers, A. Van Amerongen, L. Fukal, and P. Rauch. 2009. Nucleic acid lateral flow immunoassay for the detection of pathogenic bacteria from food. *Czech Journal of Food Sciences* 27: S350–S353. <https://doi.org/10.17221/959-CJFS>.
- Castellanos-Gonzalez, A., T.R. Shelite, N. Lloyd, A. Sadiqova, R. Ping, N. Williams-Bouyer, P.C. Melby, and B.L. Travi. 2021. Direct RT-PCR amplification of SARS-CoV-2 from clinical samples using a concentrated viral lysis-amplification buffer prepared with IGEPAL-630. *Scientific Reports* 11 (1): 14204. <https://doi.org/10.1038/s41598-021-93333-2>.
- Chua, K.B., W.J. Bellini, P.A. Rota, B.H. Harcourt, A. Tamin, S. Lam, T.G. Ksiazek, P.E. Rollin, S.R. Zaki, W.J. Shieh, et al. 2000. Nipah virus: A recently emergent deadly paramyxovirus. *Science* 288: 1432–1435. <https://doi.org/10.1126/science.288.5470.1432>.

- Corman, V.M., I. Eckerle, T. Bleicker, A. Zaki, O. Landt, M. Eschbach-Bludau, S. van Boheemen, R. Gopal, M. Ballhause, T.M. Bestebroer, et al. 2012. Detection of a novel human coronavirus by real-time reverse-transcription polymerase chain reaction. *Eurosurveillance* 17: 20285. <https://doi.org/10.2807/ese.17.39.20285-en>.
- Crannell, Z., A. Castellanos-Gonzalez, G. Nair, R. Mejia, A.C. White, and R. Richards-Kortum. 2016. Multiplexed recombinase polymerase amplification assay to detect intestinal protozoa. *Analytical Chemistry* 88 (3): 1610–1616. <https://doi.org/10.1021/acs.analchem.5b03267>.
- Damborský, P., K.M. Koczula, A. Gallotta, and J. Katrlík. 2016. Lectin-based lateral flow assay: Proof-of-concept. *The Analyst* 141: 6444–6448. <https://doi.org/10.1039/c6an01746k>.
- Demetria, C., I. Smith, T. Tan, D. Villarico, E.M. Simon, R. Centeno, M. Tachedjian, S. Taniguchi, M. Shimojima, N.L.J. Miranda, et al. 2018. Reemergence of reston ebolavirus in cynomolgus monkeys, the Philippines, 2015. *Emerging Infectious Diseases* 24 (7): 1285–1291. <https://doi.org/10.3201/eid2407.171234>.
- Epstein, J.H., V. Prakash, C.S. Smith, P. Daszak, A.B. McLaughlin, G. Meehan, H.E. Field, and A.A. Cunningham. 2008. Henipavirus infection in fruit bats (*Pteropus giganteus*), India. *Emerging Infectious Diseases* 14: 1309–1311. <https://doi.org/10.3201/eid1408.071492>.
- Fajardo, T.V.M., M.F. Vanni, and O. Nickel. 2017. Absolute quantification of viruses by TaqMan real-time RT-PCR in grapevines. *Ciencia Rural* 47 (6): e20161063. <https://doi.org/10.1590/0103-8478cr20161063>.
- Geldenhuys, M., J. Weyer, L.H. Nel, and W. Markotter. 2013. Coronaviruses in South African bats. *Vector-Borne and Zoonotic Diseases* 13: 516–519. <https://doi.org/10.1089/vbz.2012.1101>.
- Hall, A.T., A.M. Zovanyi, D.R. Christensen, J.W. Koehler, and T. Devins Minogue. 2013. Evaluation of inhibitor-resistant real-time PCR methods for diagnostics in clinical and environmental samples. *PLoS One* 8 (9): e73845. <https://doi.org/10.1371/journal.pone.0073845>.
- Halpin, K., A.D. Hyatt, R. Fogarty, D. Middleton, J. Bingham, J.H. Epstein, S.A. Rahman, T. Hughes, C. Smith, H.E. Field, P. Daszak, the Henipavirus Ecology Research Group. 2011. Pteropid bats are confirmed as the reservoir hosts of henipaviruses: A comprehensive experimental study of virus transmission. *American Journal of Tropical Medicine and Hygiene* 85 (5): 946–951. <https://doi.org/10.4269/ajtmh.2011.10-0567>.
- Ithete, N.L., S. Stoffberg, V.M. Corman, V.M. Cottontail, L.R. Richards, S. Schoeman, C. Drosten, J.F. Drexler, and W. Preiser. 2013. Close relative of human Middle East respiratory syndrome coronavirus in bat, South Africa. *Emerging Infectious Diseases* 19 (10): 1697–1699. <https://doi.org/10.3201/eid1910.130946>.
- James, H.E., K. Ebert, R. McGonigle, S.M. Reid, N. Boonham, J.A. Tomlinson, G.H. Hutchings, M. Denyer, C.A.L. Oura, and J.P. Dukes. 2010. Detection of African swine fever virus by loop-mediated isothermal amplification. *The Journal of Virological Methods* 164 (1–2): 68–74. <https://doi.org/10.1016/j.jviro.2009.11.034>.
- Jayme, S.I., H.E. Field, C. Jong, K.J. Olival, G. Marsh, A.M. Tagtag, T. Hughes, A.C. Bucad, J. Barr, R.R. Azul, et al. 2015. Molecular evidence of Ebola Reston virus infection in Philippine bats. *Virology Journal* 12: 107. <https://doi.org/10.1186/s12985-015-0331-3>.
- Jia, Y., H. Sun, J. Tian, Q. Song, and W. Zhang. 2021. Paper-based point-of-care testing of SARS-CoV-2. *Frontiers in Bioengineering and Biotechnology* 9: 773304. <https://doi.org/10.3389/fbioe.2021.773304>.
- Kamphee, H., A. Chairprasert, T. Prammananan, N. Wiriyachaiyorn, A. Kanchanavee, and T. Dharakul. 2015. Rapid molecular detection of multidrug resistant tuberculosis by PCR-nucleic acid lateral flow immunoassay. *PLoS One* 10 (9): e0137791. <https://doi.org/10.1371/journal.pone.0137791>.
- Krölov, K., J. Frolova, O. Tudoran, J. Suhorutsenko, T. Lehto, H. Sibul, I. Mäger, M. Laanpere, I. Tulp, and U. Langel. 2014. Sensitive and rapid detection of *Chlamydia trachomatis* by recombinase polymerase amplification directly from urine samples. *The Journal of Molecular Diagnostics* 16 (1): 127–135. <https://doi.org/10.1016/j.jmoldx.2013.08.003>.
- Leroy, E.M., B. Kumulungi, X. Pourrut, P. Rouquet, A. Hassanin, and P. Yaba. 2005. Fruit bats as reservoirs of Ebola virus. *Nature* 438: 575–576. <https://doi.org/10.1038/438575a>.
- Marsh, G.A., J. Haining, R. Robinson, A. Foord, M. Yamada, J.A. Barr, J. Payne, J.Y.M. White, J. Bingham, P.E. Rollin, S.T. Nichol, L.F. Wang, and D. Middleton. 2011. Ebola Reston virus infection of pigs: Clinical significance and transmission potential. *The Journal of Infectious Diseases* 204: 804–809. <https://doi.org/10.1093/infdis/jir300>.
- Mens, P.F., A. Moers, L.M. de Bes, J. Flint, J.R. Sak, L. Keerecharoen, C. van Overmeir, J.J. Verweij, R.L. Hallett, B. Wihokhoen, et al. 2012a. Development, validation and evaluation of a rapid PCR-nucleic acid lateral flow immunoassay for the detection of Plasmodium and the differentiation between Plasmodium falciparum and Plasmodium vivax. *Malaria Journal* 11: 279. <https://doi.org/10.1186/1475-2875-11-279>.
- Mens, P.F., H.M. de Bes, P. Sondo, N. Laochan, L. Keerecharoen, A. van Amerongen, J. Flint, J.R. Sak, S. Proux, H. Tinto, and H.D. Schallig. 2012b. Direct blood PCR in combination with nucleic acid lateral flow immunoassay for detection of Plasmodium species in settings where malaria is endemic. *Journal of Clinical Microbiology* 11: 3520–3525. <https://doi.org/10.1128/JCM.01426-12>.
- Miranda, M.E., M.E. White, M.M. Dayrit, C.G. Hayes, T.G. Ksiazek, and J.P. Burans. 1991. Seroepidemiological study of filovirus related to Ebola in the Philippines. *The Lancet* 337 (8738): 425–426. [https://doi.org/10.1016/0140-6736\(91\)91199-5](https://doi.org/10.1016/0140-6736(91)91199-5).
- Mungall, B.A., D. Middleton, G. Cramer, J. Bingham, K. Halpin, G. Russell, D. Green, J. Mceachern, L.I. Pritchard, B.T. Eaton, et al. 2006. Feline model of acute nipah virus infection and protection with a soluble glycoprotein-based subunit vaccine. *Journal of Virology* 80: 12293–12302. <https://doi.org/10.1128/jvi.01619-06>.
- Posthuma-Trumpie, G.A., J. Korf, and A. van Amerongen. 2009. Lateral flow (immuno) assay: Its strengths, weaknesses, opportunities and threats – literature survey. *Analytical and Bioanalytical Chemistry* 393: 569–582. <https://doi.org/10.1007/s00216-008-2287-2>.
- Pourrut, X., M. Souris, J.S. Towner, P.E. Rollin, S.T. Nichol, J.P. Gonzalez, and E. Leroy. 2009. Large serological survey showing cocirculation of Ebola and Marburg viruses in Gabonese bat populations, and a high seroprevalence of both viruses in Rousettus aegyptiacus. *BMC Infectious Diseases* 9: 159. <https://doi.org/10.1186/1471-2334-9-159>.
- Shaopeng, W., D. Tian, S. Hongxia, Q. Kun, Ye. Jianqiang, and Q. Aijian. 2023. A quadruplex real-time PCR assay combined with a conventional PCR for the differential detection of Marek's disease virus vaccines and field strains. *Frontiers in Veterinary Science* 10: 2297–1769. <https://doi.org/10.3389/fvets.2023.1161441>.
- Smyrliak, I., M. Ekman, A. Lentini, N. Rufino de Sousa, N. Papanicolaou, M. Vondracek, J. Aarum, H. Safari, S. Muradrasoli, A.G. Rothfuchs, J. Albert, B. Högberg, and B. Reinius. 2020. Massive and rapid COVID-19 testing is feasible by extraction-free SARS-CoV-2 RT-PCR. *Nature Communications* 11: 4812. <https://doi.org/10.1038/s41467-020-18611-5>.
- Taniguchi, S., S. Watanabe, J.S. Masangkay, T. Omatsu, T. Ikegami, P. Alviola, N. Ueda, K. Iha, H. Fujii, Y. Ishii, et al. 2011. Reston Ebolavirus antibodies in bats, the Philippines. *Emerging Infectious Diseases* 17 (8): 1559–1560. <https://doi.org/10.3201/eid1708.101693>.
- Trevethan, R. 2017. Sensitivity, specificity, and predictive values: Foundations, pliabilitys, and pitfalls in research and practice. *Frontiers in Public Health* 5: 307. <https://doi.org/10.3389/fpubh.2017.00307>.
- Trombley, A.R., L. Wachter, J. Garrison, V. Buckley-Beason, J. Jahrling, L. Hensley, R.J. Schoepp, D.A. Norwood, A. Goba, J. Fair, and D. Kulesh. 2010. Comprehensive panel of real-time TaqMan polymerase chain reaction assays for detection and absolute quantification of filoviruses, arenaviruses, and new world hantaviruses. *American Journal of Tropical Medicine and Hygiene* 82: 954–960. <https://doi.org/10.4269/ajtmh.2010.09-0636>.
- Yadav, P.D., C.G. Raut, A.M. Shete, A.C. Mishra, J.S. Towner, S.T. Nichol, and D.T. Mourya. 2012. Short report: Detection of Nipah virus RNA in fruit bat (*Pteropus giganteus*) from India. *American Journal of Tropical Medicine and Hygiene* 87: 576–578. <https://doi.org/10.4269/ajtmh.2012.11-0416>.
- Yadav, P., A. Sudeep, M. Gokhale, S. Pawar, A. Shete, D. Patil, V. Kumar, R. Lakra, P. Sarkale, S. Nichol, and D. Mourya. 2018. Circulation of Nipah virus in *Pteropus giganteus* bats in northeast region of India, 2015. *The Indian Journal of Medical Research* 147: 318–320. https://doi.org/10.4103/ijmr.IJMR_1488_16.
- Yadav, P.D., A.M. Shete, G. Kumar, P. Sarkale, R.R. Sahay, C. Radhakrishnan, R. Lakra, P. Pardeshi, N. Gupta, R.R. Gangakhedkar, V.R. Rajendran, R. Sadanandan, and D.T. Mourya. 2019. Nipah virus sequences from humans and bats during Nipah outbreak, Kerala, India, 2018. *Emerging Infectious Diseases* 25 (5): 1003–1006. <https://doi.org/10.3201/eid2505.181076>.
- Yang, L.W.Z., X. Ren, F. Yang, J. Zhang, G. He, J. Dong, L. Sun, Y. Zhu, S. Zhang, and Q. Jin. 2014. MERS-related betacoronavirus in *Vespertilio superans* bats, China. *Emerging Infectious Diseases* 20 (7): 1260–1262. <https://doi.org/10.3201/eid2007.140318>.

- Zaki, A.M., S. van Boheemen, T.M. Bestebroer, A.D. Osterhaus, and R.A. Fouchier. 2012. Isolation of a novel coronavirus from a man with pneumonia in Saudi Arabia. *New England Journal of Medicine* 367 (19): 1814–1820. <https://doi.org/10.1056/NEJMoa1211721>.
- Zhang, A.N., Y. Mao, and T. Zhang. 2016. Development of quantitative real-time PCR assays for different clades of "Candidatus Accumulibacter." *Scientific Reports* 6: 23993. <https://doi.org/10.1038/srep23993>.
- Zhang, C., T. Zheng, H. Wang, W. Chen, X. Huang, J. Liang, L. Qiu, D. Han, and W. Tan. 2021. Rapid one-pot detection of SARS-CoV-2 based on a lateral flow assay in clinical samples. *Analytical Chemistry* 93 (7): 3325–3330. <https://doi.org/10.1021/acs.analchem.0c05059>.
- Zhu, X., X. Wang, L. Han, T. Chen, L. Wang, H. Li, S. Li, L. He, X. Fu, S. Chen, M. Xing, H. Chen, and Y. Wang. 2020. Multiplex reverse transcription loop-mediated isothermal amplification combined with nanoparticle-based lateral flow biosensor for the diagnosis of COVID-19. *Biosensors and Bioelectronics* 166: 112437. <https://doi.org/10.1016/j.bios.2020.112437>.

Publisher's Note

Springer Nature remains neutral with regard to jurisdictional claims in published maps and institutional affiliations.